Share Your Innovations through JACS Directory

Journal of Nanoscience and Technology

Visit Journal at http://www.jacsdirectory.com/jnst

ISSN: 2455-0191

Synthesis and Characterization of Co_3O_4-ZnO-ZrO_2 Ternary Nanoparticles

S. Alwin David, V. Veeraputhiran, C. Vedhi*

Department of Chemistry, V.O. Chidambaram College, Tuticorin – 628 008, Tamil Nadu, India.

ARTICLE DETAILS

Article history:
Received 05 November 2017
Accepted 21 November 2017
Available online 22 November 2017

Keywords:
Co_3O_4-ZnO-ZrO_2 NPs
Mixed Nano Oxides
Wet Chemical Method
Band Gap Energy

ABSTRACT

Nano Co_3O_4-ZnO-ZrO_2 mixed metal oxides were synthesized by wet chemical method by mixing of equimolar solutions of cobalt chloride, zinc sulfate and zirconium oxychloride in aqueous sodium hydroxide and refluxed at elevated temperature. The synthesized mixed nano oxides were characterized by FT-IR, XRD, UV-Vis DRS, TEM, SAED, SEM, EDAX and AFM. The FTIR spectra exposed the presence of M-O bonds (M = Co, Zn, Zr). From XRD studies, the size of the Co_3O_4-ZnO-ZrO_2 NPs are found to be 28.11 – 52.36 nm through Scherrer's formula. The XRD patterns also reveal that the particle size is drastically increased with increasing concentration of precursors. From UV-Vis diffuse reflectance spectra (DRS), band gap energies of the (0.1 – 0.5 M) Co_3O_4-ZnO-ZrO_2 NPs are found to be in the range of 2.41-2.68 eV. The TEM, SEM and AFM micrographs of 0.1 M Co_3O_4-ZnO-ZrO_2 NPs display irregular shape with size ranging from 20-45 nm. SAED pattern confirms the crystalline nature of these nanoparticles. EDAX analysis indicates the presence of Co, Zn, Zr and O.

1. Introduction

Large surface-to-volume ratio and small size of the nanoparticles can guide to the different physical and chemical properties which are altered from those of their bulk counterparts. In recent times, there has been increasing attention in the synthesis of nano mixed metal oxides. Co_3O_4 is an important p-type semiconductor which has been widely used in supercapacitor, lithium-ion batteries, solar cells, electrocatalysis, photocatalysis and sensing devices [1, 2]. ZnO is one of the most widely utilized n-type semiconductor due to its applications in UV-light emitting diodes, piezo-electric transducers, solar cells, memory devices, photodiodes, photodetectors, light emitting diodes, anticancer therapeutic agent, sensors, industrial wastewater treatment and photocatalysis [3, 4]. ZrO_2 is a noteworthy n-type semiconductor because of its applications in many fields such as high temperature ceramics, restorative dentistry, electrochemical capacitor electrodes, sensor, fuel cells, optical devices and photocatalysis [5, 6].

Therefore, the research limelight has twisted towards reasonably priced metal oxides such as Co_3O_4, ZnO and ZrO_2. In this work, Co_3O_4-ZnO-ZrO_2 NPs were obtained by wet chemical method. The synthesized ternary metal oxide nanomaterials were characterized by FT-IR, XRD, DRS, TEM, SAED, SEM, EDAX and AFM.

2. Experimental Methods

2.1 Materials

The precursors $CoCl_2.6H_2O$, $ZnSO_4.7H_2O$, $ZrOCl_2.8H_2O$ and the precipitant (NaOH) were purchased from Merck. All solutions were prepared using deionized water.

2.2 Synthesis of Co_3O_4-ZnO-ZrO_2 Nanoparticles

About 25 mL of 0.1 M $CoCl_2.6H_2O$ was added to the aqueous solution of 75 mL of 1.0 M NaOH solution and stirred well. To this mixture 25 mL of 0.1 M $ZnSO_4.7H_2O$ and 25 mL of 0.1 M $ZrOCl_2.8H_2O$ were added. The resulting mixture was stirred well and refluxed at an elevated temperature for 3 hours. The product was filtered, washed with water and dried. Similar procedure was carried out to synthesize different concentrations of (0.2 M - 0.5 M) Co_3O_4-ZnO-ZrO_2 nanoparticles.

2.3 Characterization

FTIR measurements of samples prepared as KBr disks were performed on a Thermo Scientific Nicolet iS5 FTIR spectrometer. The average particle size of nanoparticles was determined by XPERT-PRO X-ray diffractometer using CuKα radiation. UV-Vis diffuse reflectance spectra were recorded with Jasco V-600 spectrophotometer. Philips-CM200 Transmission Electron Microscopy (TEM) was used to study the shape, particle size and lattice image of the nanoparticles. The morphology and composition of the nanoparticles were determined by JEOL JSM 6390 Scanning Electron Microscopy (SEM) with EDAX. Atomic force microscopy (AFM) images were recorded on a Nanosurf Easyscan 2 AFM instrument to obtain topographical images of the nanoparticles.

3. Results and Discussion

3.1 FTIR Analysis

FTIR spectra of Co_3O_4-ZnO-ZrO_2 NPs are shown in Fig. 1. The bands in the low frequency region, 568–962 cm^{-1} correspond to the lattice vibration modes of M-O (M = Co, Zn, Zr) [7, 8]. IR bands observed at around 1113 – 1116 cm^{-1} are due to the presence of Symmetric stretching of Zr-O [8].

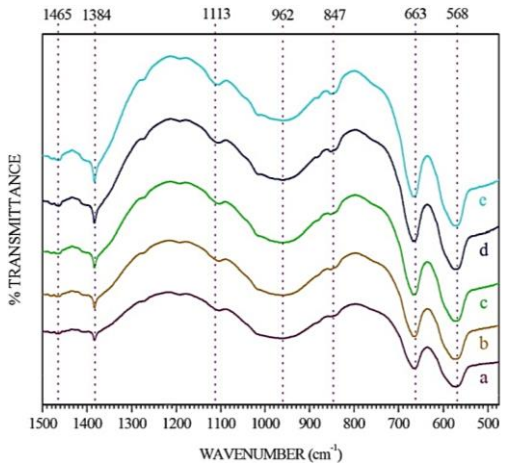

Fig. 1 FTIR Spectra of a) 0.1 M Co_3O_4-ZnO-ZrO_2 NPs b) 0.2 M Co_3O_4-ZnO-ZrO_2 NPs c) 0.3 M Co_3O_4-ZnO-ZrO_2 NPs d) 0.4 M Co_3O_4-ZnO-ZrO_2 NPs and e) 0.5 M Co_3O_4-ZnO-ZrO_2 NPs

*Corresponding Author
Email Address: cvedhi23@gmail.com(C. Vedhi)

The band appears at 1384 cm^{-1} in the FTIR spectra indicates the presence of M-O rocking in plane vibration (M = Co, Zn, Zr) [9]. The absorption peaks at around 1465 cm^{-1} are assigned to the stretching vibration of Co–O bond [10].

3.2 XRD Analysis

The XRD patterns of the Co_3O_4-ZnO-ZrO_2 NPs are presented in Fig. 2, the diffraction peaks at 2θ values of 19.18°, 31.90°, 36.35°, 38.25° and 56.13° are attributed to (111), (220), (311), (222) and (422) planes of Co_3O_4 (JCPDS card no. 76-1802) respectively [11]. The diffraction peaks at 2θ values of 32.94°, 47.75°, 62.94° and 68.06° are due to (002), (102), (103) and (112) planes of ZnO (JCPDS card no. 36-1451) respectively [12]. The diffraction peaks at 2θ values of 35.10°, 51.15° and 58.97° are assigned to (200), (220) and (311) planes of ZrO_2 (JCPDS card no. 50-1089) respectively [5].

Similar diffraction peaks are also observed in all the samples as given in the Fig. 2. The average particle sizes of the Co_3O_4-ZnO-ZrO_2 NPs as estimated using the Scherrer's formula are in the range of 28.11–52.36 nm. As the concentration of the precursors increases from 0.1 M to 0.5 M, the size of the nanoparticles also increases to an extent due to agglomeration of the small metal oxide nanoparticles.

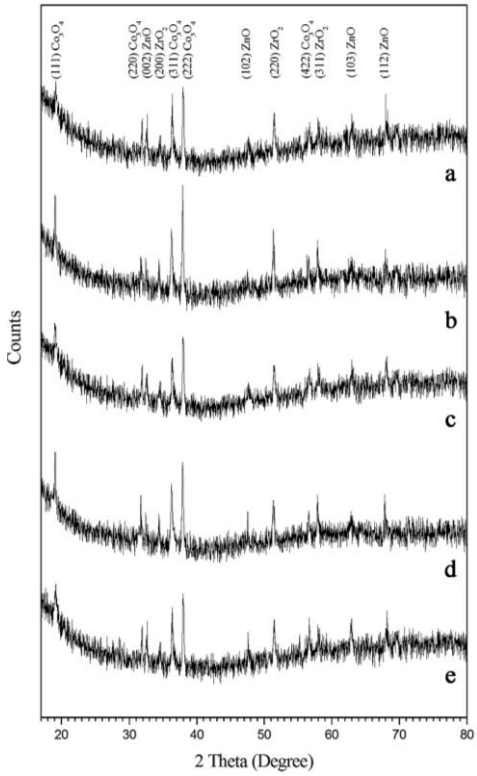

Fig. 2 XRD Patterns of a) 0.1 M Co_3O_4-ZnO-ZrO_2 NPs b) 0.2 M Co_3O_4-ZnO-ZrO_2 NPs c) 0.3 M Co_3O_4-ZnO-ZrO_2 NPs d) 0.4 M Co_3O_4-ZnO-ZrO_2 NPs and e) 0.5 M Co_3O_4-ZnO-ZrO_2 NPs

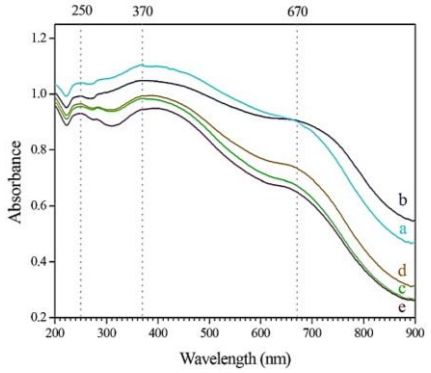

Fig. 3 UV-Visible diffuse reflectance spectra of a) 0.1 M Co_3O_4-ZnO-ZrO_2 NPs b) 0.2 M Co_3O_4-ZnO-ZrO_2 NPs c) 0.3 M Co_3O_4-ZnO-ZrO_2 NPs d) 0.4 M Co_3O_4-ZnO-ZrO_2 NPs and e) 0.5 M Co_3O_4-ZnO-ZrO_2 NPs

3.3 UV-Visible Diffuse Reflectance Spectroscopic Analysis

The light absorbance properties of Co_3O_4-ZnO-ZrO_2 NPs are investigated using UV-Vis diffuse reflectance spectrophotometer in the wavelength range of 200–900 nm. As shown in UV-Vis diffuse reflectance spectra (Fig. 3), two absorbance bands centered between 250-252 nm and 370–394 nm with a hump at around 670 nm, suggest that the samples can be activated by both UV and visible light irradiations [11].

There is a red shift in absorption bands (from 370 nm to 394 nm) observed in Co_3O_4-ZnO-ZrO_2 NPs (from 0.1 M to 0.5 M) synthesized. This red shift is due to the increase in the particle size as well as decrease in the inter particle distance of Co_3O_4-ZnO-ZrO_2 NPs (from 0.1 M to 0.5 M) [13].

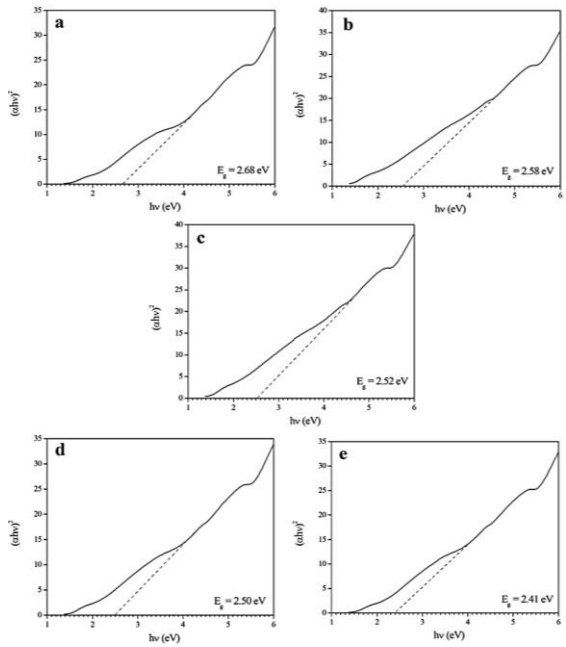

Fig. 4 Plot of $(\alpha h\nu)^2$ versus (hν) of a) 0.1 M Co_3O_4-ZnO-ZrO_2 NPs b) 0.2 M Co_3O_4-ZnO-ZrO_2 NPs c) 0.3 M Co_3O_4-ZnO-ZrO_2 NPs d) 0.4 M Co_3O_4-ZnO-ZrO_2 NPs and e) 0.5 M Co_3O_4-ZnO-ZrO_2 NPs

The band gap (E_g) of the NPs can be determined using well-known Tauc relation, $(\alpha h\nu)^n = A\ (h\nu - E_g)$, where α, h, ν and A are the absorption coefficient, Plank constant, light frequency and a constant, respectively. While n = 2 for direct inter band transition. The Eg value can be estimated by plotting $(\alpha h\nu)^2$ versus hν and extrapolating the linear part of curve to energy axis at α = 0.

The calculated band gap energies are 2.68, 2.58, 2.52, 2.50 and 2.41 eV for 0.1 M, 0.2 M, 0.3 M, 0.4 M and 0.5 M Co_3O_4-ZnO-ZrO_2 NPs, respectively. The band gap energy values suggest that these Co_3O_4-ZnO-ZrO_2 NPs are visible light sensitive, capable to be photocatalysts under visible light illumination [11].

3.4 TEM Analysis

TEM images shown in Fig. 5, reveal that Co_3O_4-ZnO-ZrO_2 NPs formed are irregular in shape and non-uniform in size ranging from 20-45 nm. It may be noted that the value obtained from TEM is in good agreement with that obtained from XRD measurements. The SAED pattern taken from the 0.1 M Co_3O_4-ZnO-ZrO_2 NPs (Fig. 5(d)) shows strong diffraction rings and associated diffraction spots that indicate the crystalline nature of these nanoparticles.

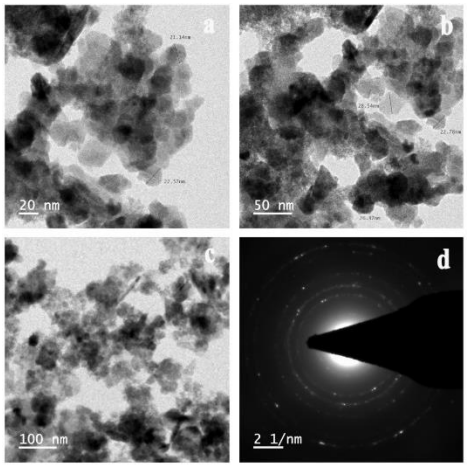

Fig. 5 TEM image of 0.1 M Co_3O_4-ZnO-ZrO_2 NPs in (a) 20 nm scale (b) 50 nm scale (c) 100 nm scale (d) SAED pattern of 0.1 M Co_3O_4-ZnO-ZrO_2 NPs

3.5 SEM Analysis

SEM micrographs of Co_3O_4-ZnO-ZrO_2 NPs synthesized at five different concentrations of $CoCl_2$, $ZnSO_4$ and $ZrOCl_2$ (0.1 M, 0.2 M, 0.3 M, 0.4 M, and 0.5 M) are shown in Fig. 6. The prepared Co_3O_4-ZnO-ZrO_2 NPs display granular appearances with some rod like morphology. The SEM micrographs also reveal that the granule size is drastically increased with increasing concentration of the precursors.

3.6 EDAX Analysis

EDAX analysis was performed to confirm the elemental composition of the synthesized Co_3O_4-ZnO-ZrO_2 NPs. The presence of cobalt (Co), zinc (Zn), zirconium (Zr) and oxygen (O) signals peaks in the EDAX spectrum confirms that the metal oxides are dispersed well in Co_3O_4-ZnO-ZrO_2 NPs (Fig. 6f). The atomic percent of Co, Zn and Zr is 9.85, 8.20 and 9.51 respectively. Obviously, the atomic ratio of Co, Zn and Zr is close to their molar ratio of their precursor (1:1:1) in the synthetic procedure.

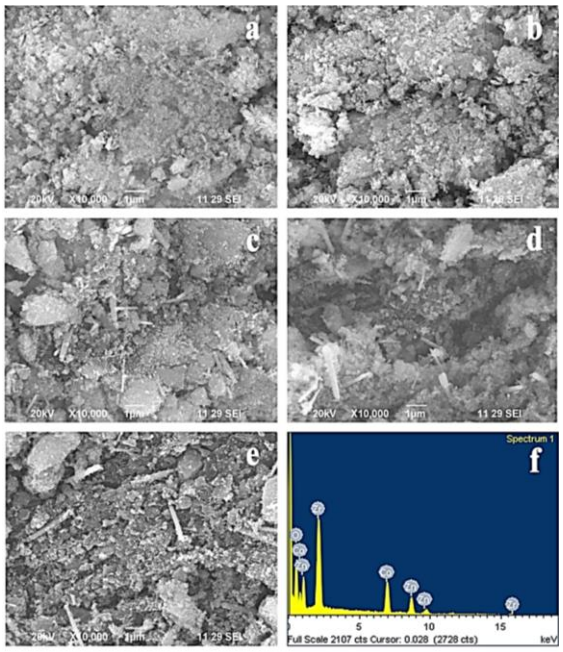

Fig. 6 SEM image of a) 0.1 M Co_3O_4-ZnO-ZrO_2 NPs b) 0.2 M Co_3O_4-ZnO-ZrO_2 NPs c) 0.3 M Co_3O_4-ZnO-ZrO_2 NPs d) 0.4 M Co_3O_4-ZnO-ZrO_2 NPs and e) 0.5 M Co_3O_4-ZnO-ZrO_2 NPs

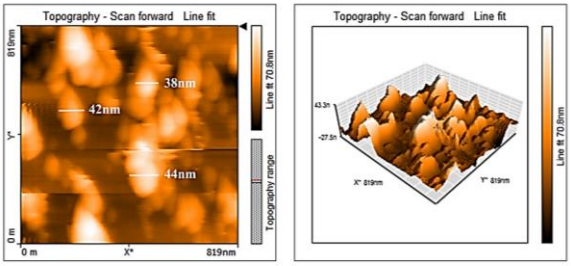

Fig. 7 AFM images of 0.1 M Co_3O_4-ZnO-ZrO_2 NPs

3.7 AFM Analysis

The AFM images that illustrate the surface morphology and roughness of Co_3O_4-ZnO-ZrO_2 NPs are shown in Fig. 7. The shape of Co_3O_4-ZnO-ZrO_2 NPs is irregular elongated sphere and the size is in the range of 20-45 nm. From the surface roughness analysis, it is observed that the surface roughness of the Co_3O_4-ZnO-ZrO_2 NPs is estimated to be about 11.442 nm for the root mean square roughness (S_q) and 8.877 nm for the average surface roughness (S_a).

4. Conclusion

Nano Co_3O_4-ZnO-ZrO_2 mixed oxides were synthesized effectively by wet chemical process. XRD patterns and SAED confirm the crystalline nature of Co_3O_4-ZnO-ZrO_2 NPs with average particle size of 28.11–52.36 nm. Co_3O_4-ZnO-ZrO_2 NPs are found to be irregular in shape with variable size ranging from 20 - 45nm, as apparent by SEM, TEM and AFM. The band gap energies for the Co_3O_4-ZnO-ZrO_2 NPs are found to be 3.15 -3.35 eV.

References

[1] Y. Wang, W. Wang, W. Song, Binary CuO/Co_3O_4 nanofibers for ultrafast and amplified electrochemical sensing of fructose, Electrochim. Acta 56 (2011) 10191-10196.
[2] T.K. Jana, A. Pal, K. Chatterjee, Magnetic and photocatalytic study of Co_3O_4–ZnO nanocomposite, Jour. Alloys Comp. 653 (2015) 338-344.
[3] S. Akir, A. Barras, Y. Coffinier, M. Bououdina, R. Boukherroub, A.D. Omrani, Eco-friendly synthesis of ZnO nanoparticles with different morphologies and their visible light photocatalytic performance for the degradation of Rhodamine B, Ceram. Int. 42 (2016) 10259-10265.
[4] L. Fu, Z. Fu, *Plectranthus amboinicus* leaf extract–assisted biosynthesis of ZnO nanoparticles and their photocatalytic activity, Ceram. Int. 41 (2015) 2492–2496.
[5] N.C.S. Selvam, A. Manikandan, L.J. Kennedy, J.J. Vijaya, Comparative investigation of zirconium oxide (ZrO_2) nano and microstructures for structural, optical and photocatalytic properties, J. Colloid Interf. Sci. 389 (2013) 91-98.
[6] S.Z. Ajabshir, M.S. Niasari, Facile route to synthesize zirconium dioxide (ZrO_2) nanostructures: Structural, optical and photocatalytic studies, Jour. Mol. Liquids 216 (2016) 545-551.
[7] M.A. Subhan, T. Ahmed, Synthesis, characterization and spectroscopic investigations of novel nano multi-metal oxide Co_3O_4-CeO_2-ZnO, Spectrochim. Acta A: Mol. Biomol. Spect. 129 (2014) 377-381.
[8] R.R. Muthuchudarkodi, C. Vedhi, Synthesis and characterization of nano CuO–ZrO_2 mixed oxide, Adv. Mater. Res. 678 (2013) 50-55.
[9] K.J. Arun, A.K. Batra, A. Krishna, K. Bhat, M.D. Aggarwal, P.J.J. Francis, Surfactant free hydrothermal synthesis of copper oxide nanoparticles, Am. Jour. Mater. Sci. 5 (2015) 36-38.
[10] R.A. Tuwirqi, A.A.A. Ghamdi, N.A. Aal, A. Umar, W.E. Mahmoud, Facile synthesis and optical properties of Co_3O_4 nanostructures by the microwave route, Superlattice. Microst. 49 (2011) 416-421.
[11] Y. Wang, L. Zhou, X. Duan, H. Sun, E.L. Tin, W. Jin, S. Wang, Photochemical degradation of phenol solutions on Co_3O_4 nanorods with sulfate radicals, Catal. Today 258 (2015) 576-584.
[12] P. Worajittiphon, K. Pingmuang, B. Inceesungvorn, N. Wetchakun, S. Phanichphant, Enhancing the photocatalytic activity of ZnO nanoparticles for efficient rhodamine B degradation by functionalized grapheme nanoplatelets, Ceram. Int. 41 (2015) 1885-1889.
[13] S.A. David, K.M. Ponvel, M.A. Fathima, S. Anita, J. Ashli, A. Athilakshmi, Biosynthesis of silver nanoparticles by *Momordica charantia* leaf extract: Characterization and their antimicrobial activities, J. Nat. Prod. Plant Resour. 4 (2014) 1-8.